

# An Analysis of RF Transfer Learning Behavior Using Synthetic Data

Lauren J. Wong<sup>1,2,3\*</sup> , Sean McPherson<sup>3</sup> , and Alan J. Michaels<sup>1,2</sup> 

<sup>1</sup> Hume Center for National Security and Technology, Virginia Tech

<sup>2</sup> Bradley Department of Electrical and Computer Engineering, Virginia Tech

<sup>3</sup> Intel AI Lab, Santa Clara, CA

\* Correspondence: ljwong@vt.edu

**Abstract:** Transfer learning (TL) techniques, which leverage prior knowledge gained from data with different distributions to achieve higher performance and reduced training time, are often used in computer vision (CV) and natural language processing (NLP), but have yet to be fully utilized in the field of radio frequency machine learning (RFML). This work systematically evaluates how radio frequency (RF) TL behavior by examining how the training domain and task, characterized by the transmitter/receiver hardware and channel environment, impact RF TL performance for an example automatic modulation classification (AMC) use-case. Through exhaustive experimentation using carefully curated synthetic datasets with varying signal types, signal-to-noise ratios (SNRs), and frequency offsets (FOs), generalized conclusions are drawn regarding how best to use RF TL techniques for domain adaptation and sequential learning. Consistent with trends identified in other modalities, results show that RF TL performance is highly dependent on the similarity between the source and target domains/tasks. Results also discuss the impacts of channel environment, hardware variations, and domain/task difficulty on RF TL performance, and compare RF TL performance using head re-training and model fine-tuning methods.

**Keywords:** machine learning, deep learning, transfer learning, radio frequency machine learning

## 1. Introduction

Radio frequency machine learning (RFML) is loosely defined as the application of deep learning (DL) to raw RF data, and has yielded state-of-the-art algorithms for spectrum awareness, cognitive radio, and networking tasks. Existing RFML works have delivered increased performance and flexibility, and reduced the need for pre-processing and expert-defined feature extraction techniques. As a result, RFML is expected to enable greater efficiency, lower latency, and better spectrum efficiency in 6G systems [1]. However, to date, little research has considered and evaluated the performance of these algorithms in the presence of changing hardware platforms and channel environments, adversarial contexts, or resource constraints that are likely to be encountered in real-world systems [2].

Current state-of-the-art RFML techniques rely upon supervised learning techniques trained from random initialization, and thereby assume the availability of a large corpus of labeled training data (synthetic, captured, or augmented [3]), which is representative of the anticipated deployed environment. Over time, this assumption inevitably breaks down as a result of changing hardware and channel conditions, and as a consequence, performance degrades significantly [4,5]. TL techniques can be used to mitigate these performance degradations by using prior knowledge obtained from a *source* domain and task, in the form of learned representations, to improve performance on a “similar” *target* domain and task using less data, as depicted in Fig. 1.

Though TL techniques have demonstrated significant benefits in fields such as CV and NLP [6], including higher performing models, significantly less training time, and far fewer training samples [7], [8] showed that the use of TL in RFML is currently lacking through the



**Citation:** Wong L.J.; McPherson S; Michaels A.J. An Analysis of RF Transfer Learning Behavior Using Synthetic Data. *Preprints* 2022, 1, 0. <https://doi.org/>

**Publisher’s Note:** MDPI stays neutral with regard to jurisdictional claims in published maps and institutional affiliations.



**Copyright:** © 2022 by the authors. Licensee MDPI, Basel, Switzerland. This article is an open access article distributed under the terms and conditions of the Creative Commons Attribution (CC BY) license (<https://creativecommons.org/licenses/by/4.0/>).

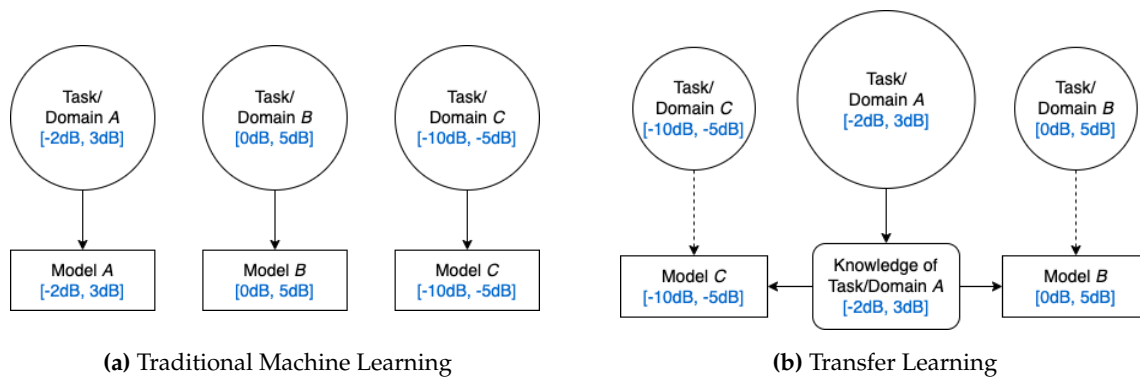


**Figure 1.** In traditional machine learning (ML) (Fig. 1a), a new model is trained from random initialization for each domain/task pairing. TL (Fig. 1b) utilizes prior knowledge learned on one domain/task, in the form of a pre-trained model, to improve performance on a second domain and/or task. A concrete example for environmental adaptation to SNR is given in blue.

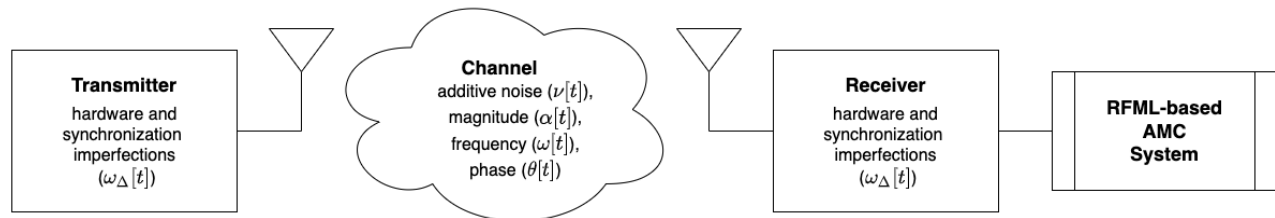


**Figure 2.** A system overview of the RF hardware and channel environment simulated in this work with the parameters/variables ( $\alpha[t]$ ,  $\omega[t]$ ,  $\theta[t]$ ,  $\nu[t]$ ,  $\omega_{\Delta}[t]$ ) that each component of the system has the most significant impact on.

construction of an RFML specific TL taxonomy. This work begins to address current limitations in understanding how the training domain and task impact learned behavior and therefore facilitate or prevent successful transfer, where the training domain is characterized by the RF hardware and the channel environment [8] depicted in Fig. 2 and the training task is the application being addressed including the range of possible outputs (i.e. the modulation schemes classified). More specifically, this work systematically evaluates RF TL performance, as measured by post-transfer top-1 accuracy, as a function of several parameters of interest for an AMC use-case [4] using synthetic datasets. First, RF domain adaptation performance is examined as a function of

- SNR, which represents an *environment adaptation* problem characterized by a change in the RF channel environment (i.e., an increase/decrease in the additive interference,  $\nu[t]$ , of the channel) and/or transmitting devices (i.e., an increases/decrease in the magnitude,  $\alpha[t]$ , of the transmitted signal),
- FO, which represents a *platform adaptation* problem characterized by a change in the transmitting and/or receiving devices (i.e., an increase/decrease in  $\omega_{\Delta}[t]$  due to hardware imperfections or a lack of synchronization), and
- Both SNR and FO, representing an *environment platform co-adaptation* problem characterized by a change in both the RF channel environment *and* the transmitting/receiving devices.

Parameter sweeps over these three scenarios addresses each type of RF domain adaptation discussed in the RFML TL taxonomy [8], and resulted in the construction of 81 training sets, 81 validation sets, and 81 test sets and the training and evaluation of 4360 models. Additionally, RF sequential learning performance is evaluated across broad categories of modulation types, namely linear, frequency-shifted, and analog modulation schemes, as well as in a successive

model refinement scenario, where a single modulation type is added/removed from the source dataset. These experiments resulted in an additional 17 training sets, 17 validation sets, and 17 test sets, and the training and evaluation of 304 models. From these experiments, we identify a number of practical takeaways for how best to utilize TL in an RFML setting including how changes in SNR and FO impact the difficulty of AMC and a comparison of head re-training versus fine-tuning for RF TL. These takeaways serve as initial guidelines for RF TL, subject to further experimentation using additional signal types, channel models, use-cases, model architectures, and augmented or captured datasets.

This paper is organized as follows: Section 2 provides requisite background knowledge of TL and RFML. In Section 3, each of the key methods and systems used and developed for this work are described in detail, including the simulation environment and dataset creation, as well as the model architecture and training. Section 4 presents experimental results and analysis, addressing the key research questions described above. Finally, Section 5 offers conclusions about the effectiveness of TL for RFML and next steps for incorporating and extending TL techniques in RFML-based research. A list of the acronyms used in this work is provided in the appendix for reference.

## 2. Background

The following subsections provide an overview of RFML, TL, and TL for RFML to provide context for the work performed herein.

### 2.1. Radio Frequency Machine Learning (RFML)

The term RFML is often used in the literature to describe any application of machine learning (ML) or DL to the RF domain. However, RFML was coined by Defense Advanced Research Projects Agency (DARPA) and defined as systems that:

- Autonomously learn features from raw data to detect, characterize, and identify signals-of-interest,
- Can autonomously configure RF sensors or communications platforms for changing communications environments, and
- Can synthesize “any possible waveform” [9].

Therefore, RFML algorithms typically utilize raw RF data as input to ML/DL techniques; most often deep neural networks (DNNs).

To date, most RFML research has focused on delivering state-of-the-art performance on spectrum awareness and cognitive radio tasks, whether through increased accuracy, increased adaptability, or using less expert knowledge. Such spectrum awareness cognitive radio tasks include signal detection, signal classification or AMC, specific emitter identification (SEI), channel modeling/emulation, positioning/localization, and spectrum anomaly detection [2]. One of the most common and arguably the most mature spectrum awareness or cognitive radio applications explored in the literature is AMC, and as such, AMC is the example use-case in this work. AMC is the task of identifying the type of or format of a detected signal, and is a key step in receiving RF signals. Traditional AMC techniques have typically consisted of an expert-defined feature extraction stage and a pattern recognition stage using techniques such as decision trees, support vector machines, and multi-layer perceptrons (MLPs) [10]. RFML-based approaches aim to both automatically learn and identify key features within signals-of-interest, as well as utilize those features to classify the signal, using only minimally pre-processed raw RF as input to DNN architectures including convolutional neural networks (CNNs) and recurrent neural networks (RNNs) [11].

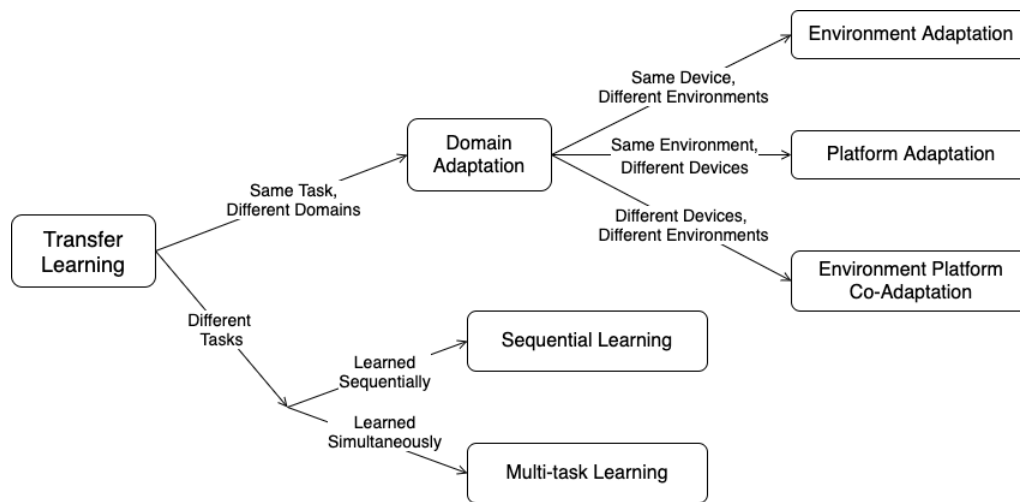


Figure 3. The RF TL taxonomy proposed in [8].

## 2.2. Transfer Learning (TL) for RFML

As previously mentioned, TL aims to utilize prior knowledge gained from a source domain/task to improve performance on a “similar” target domain/task, where training data may be limited. The domain,  $D = \{X, P(X)\}$ , consists of the input data  $X$  and the marginal probability distribution over the data  $P(X)$ . Meanwhile, the task,  $T = \{Y, P(Y|X)\}$ , consists of the label space  $Y$ , and the conditional probability distribution  $P(Y|X)$  learned from the training data pairs  $\{x_i, y_i\}$  such that  $x_i \in X$  and  $y_i \in Y$ . In the context of RFML, the domain is characterized by the RF hardware and channel environments (i.e. In-phase/Quadrature (IQ) imbalance, non-linear distortion, SNR, multi-path effects), and the task is the application being addressed, including the range of possible outputs (i.e.  $n$ -class AMC, SEI, SNR estimation).

Recent work presented the RF-specific TL taxonomy shown in Fig. 3 [8], adapted from the general TL taxonomy of [12] and the NLP-specific taxonomy of [6]. Per this taxonomy, RF TL is categorized by training data availability and whether or not the source and target tasks differ:

- Domain adaptation is the setting in which source and target tasks are the same, but the source and target domains differ, and can be further categorized as
  - Environment adaptation, where the channel environment is changing, but the transmitter/receiver pair(s) are constant,
  - Platform adaptation, where the transmitter/receiver hardware is changing, but the channel environment is consistent, and
  - Environment platform co-adaptation, where changes in both the channel environment and transmitter/receiver hardware must be overcome.
- Multi-task learning is the setting in which different source and target tasks are learned simultaneously.
- Sequential learning is the setting in which a source task is learned first, and the target task, different from the source task, is learned during a second training phase.

Typically, the same training techniques are used to perform both domain adaptation and sequential learning, most commonly head re-training and model fine-tuning, which are the focus of in this work. Existing works have successfully utilized such techniques to overcome changes in channel environment [13,14] and wireless protocol [15,16], to transfer from synthetic data to captured data [17–20], and to add or remove output classes [21], for a variety of RFML

use-cases. Meanwhile, multi-task learning approaches tend to utilize more than one loss term during a single training phase, and has been more commonly used in the context of ML-enabled wireless communications systems that use expert-defined features rather than raw RF data as input. However, multi-task learning techniques have been used to facilitate end-to-end communications systems [22], as well as to improve the explainability and accuracy of RFML models [23,24]. A systematic examination and evaluation of multi-task learning performance is left for future work.

Outside of observing the inability of pre-trained RFML models to generalize to new domains/tasks [4,25,26], little-to-no work has examined what characteristics within RF data facilitate or restrict transfer [8]. Without such knowledge, TL algorithms for RFML are generally restricted to those borrowed from other modalities, such as CV and NLP. While correlations can be drawn between the vision or language spaces and the RF space, these parallels do not always align, and therefore algorithms designed for CV and NLP may not always be appropriate for use in RFML. For example, while CV algorithm performance is not significantly impacted by a change in the camera(s) used to collect data, so long as the image resolution remains consistent [27], work in [4] showed that a change in transmitter/receiver pairs negatively impacted performance by as much as 7%, despite the collection parameters and even the brand/models of transmitters/receivers remaining consistent. Therefore, *platform adaptation* techniques that transfer knowledge gleaned from one hardware platform (or set of platforms) to a second hardware platform (or set of platforms) are a necessity in RFML, but not in CV.

### 3. Methodology

This section presents the experimental setup used in this work, shown in Fig. 4, which includes the data and dataset creation process and the model architecture, training, and evaluation, each described in detail in the following subsections.

#### 3.1. Dataset Creation

This work used a custom synthetic dataset generation tool based off the open-source signal processing library *liquid-dsp* [28], which allowed for full control over the chosen parameters-of-interest, SNR, FO, and modulation type, and ensured accurate labelling of the training, validation, and test data. The dataset creation process, shown in Fig. 4a, begins with the construction of a large “master” dataset containing all modulation schemes and combinations of SNR and FO needed for the experiments performed (Section 3.1.2). Then, for each experiment performed herein, subsets of the data were selected from the master dataset using configuration files containing the desired metadata parameters (Sections 3.1.3 - 3.1.6). The master dataset is publicly available on IEEE DataPort [29].

##### 3.1.1. Simulation Environment

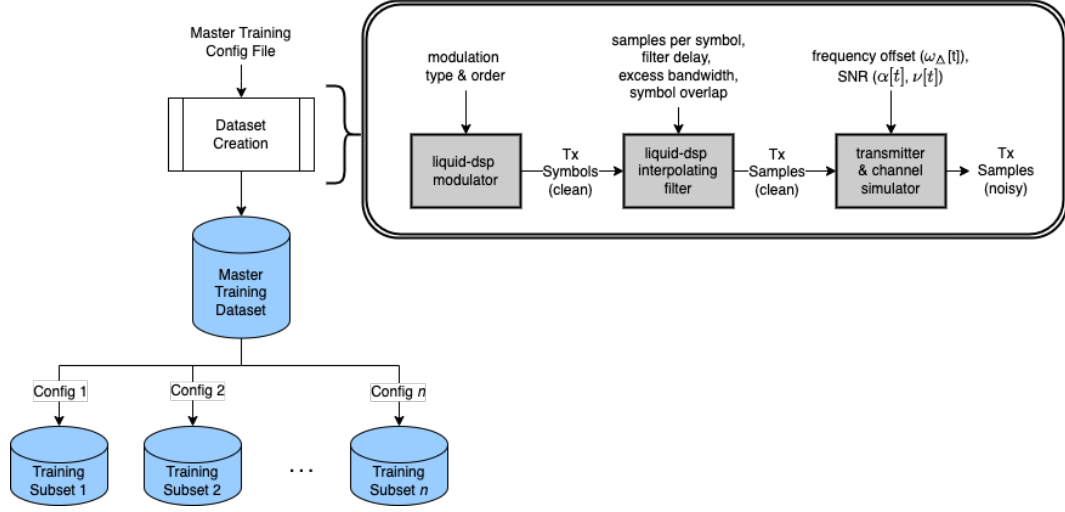
All data used in this work was generated using the same noise generation, signal parameters, and signal types as in [23]. More specifically, in this work, the signal space has been restricted to the 23 signal types shown in Table 1, observed at complex baseband in the form of discrete time-series signals,  $s[t]$ , where

$$s[t] = \alpha_{\Delta}[t] \cdot \alpha[t] e^{j\omega[t] + j\theta[t]} \cdot e^{j\omega_{\Delta}[t] + j\theta_{\Delta}[t]} + v[t] \quad (1)$$

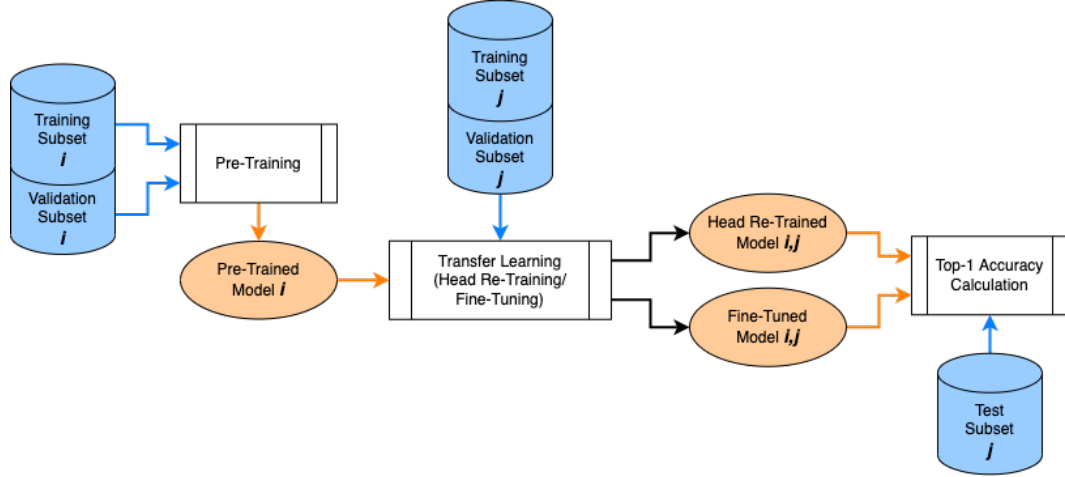
$\alpha[t]$ ,  $\omega[t]$ , and  $\theta[t]$  are the magnitude, frequency, and phase of the signal at time  $t$ , and  $v[t]$  is the additive interference from the channel. Any values subscripted with a  $\Delta$  represent imperfections/offsets caused by the transmitter/receiver and/or synchronization. Without loss of generality, all offsets caused by hardware imperfections or lack of synchronization have been consolidated onto the transmitter during simulation.

**Table 1.** Signal types included in this work and generation parameters.

Modulation Name	Parameter Space	Modulation Name	Parameter Space
BPSK	Symbol Order {2} RRC Pulse Shape Excess Bandwidth {0.35, 0.5} Symbol Overlap $\in [3, 5]$	APSK32	Symbol Order {32} RRC Pulse Shape Excess Bandwidth {0.35, 0.5} Symbol Overlap $\in [3, 5]$
QPSK	Symbol Order {4} RRC Pulse Shape Excess Bandwidth {0.35, 0.5} Symbol Overlap $\in [3, 5]$	FSK5k	Carrier Spacing {5kHz} Rect Phase Shape Symbol Overlap {1}
PSK8	Symbol Order {8} RRC Pulse Shape Excess Bandwidth {0.35, 0.5} Symbol Overlap $\in [3, 5]$	FSK75k	Carrier Spacing {75kHz} Rect Phase Shape Symbol Overlap {1}
PSK16	Symbol Order {16} RRC Pulse Shape Excess Bandwidth {0.35, 0.5} Symbol Overlap $\in [3, 5]$	GFSK5k	Carrier Spacing {5kHz} Gaussian Phase Shape Symbol Overlap {2, 3, 4} Beta $\in [0.3, 0.5]$
OQPSK	Symbol Order {4} RRC Pulse Shape Excess Bandwidth {0.35, 0.5} Symbol Overlap $\in [3, 5]$	GFSK75k	Carrier Spacing {75kHz} Gaussian Phase Shape Symbol Overlap {2, 3, 4} Beta $\in [0.3, 0.5]$
QAM16	Symbol Order {16} RRC Pulse Shape Excess Bandwidth {0.35, 0.5} Symbol Overlap $\in [3, 5]$	MSK	Carrier Spacing {2.5kHz} Rect Phase Shape Symbol Overlap {1}
QAM32	Symbol Order {32} RRC Pulse Shape Excess Bandwidth {0.35, 0.5} Symbol Overlap $\in [3, 5]$	GMSK	Carrier Spacing {2.5kHz} Gaussian Phase Shape Symbol Overlap {2, 3, 4} Beta $\in [0.3, 0.5]$
QAM64	Symbol Order {64} RRC Pulse Shape Excess Bandwidth {0.35, 0.5} Symbol Overlap $\in [3, 5]$	FM-NB	Modulation Index $\in [0.05, 0.4]$
APSK16	Symbol Order {16} RRC Pulse Shape Excess Bandwidth {0.35, 0.5} Symbol Overlap $\in [3, 5]$	FM-WB	Modulation Index $\in [0.825, 1.88]$
		AM-DSB	Modulation Index $\in [0.5, 0.9]$
		AM-DSBSC	Modulation Index $\in [0.5, 0.9]$
		AM-LSB	Modulation Index $\in [0.5, 0.9]$
		AM-USB	Modulation Index $\in [0.5, 0.9]$
		AWGN	



(a) The training dataset generation process, repeated to create the validation and test datasets.



(b) The process for model pre-training and TL.

**Figure 4.** A system overview of the (a) dataset creation and (b) model pre-training, TL, and model evaluation processes used in this work.

Signals are initially synthesized in an additive white Gaussian noise (AWGN) channel environment with unit channel gain, no phase offset, and frequency offset held constant for each observation. Like in [23], SNR is defined as

$$\text{SNR} = 10 \log_{10} \left( \frac{\sum_{t=0}^{N-1} |s[t] - v[t]|^2}{\sum_{t=0}^{N-1} |v[t]|^2} \right) \quad (2)$$

where  $N$  is the length of the capture measured in samples. This definition of SNR is based on an oracle-style knowledge of the generated signals, where the symbol energy ( $E_s$ ) has been calibrated relative to its instantaneous noise floor ( $N_0$ ), with the sampling bandwidth being marginally higher than the actual signal bandwidth. It should be noted that RFML approaches generally ingest more than one symbol at a time increasing the effective SNR. Therefore, feature estimation and/or classification is supported at lower SNRs.

In this work, we assume a blind receiver. Therefore, no synchronization or demodulation takes place. As a result, we are not limiting our conclusions by any specific filtering approaches,

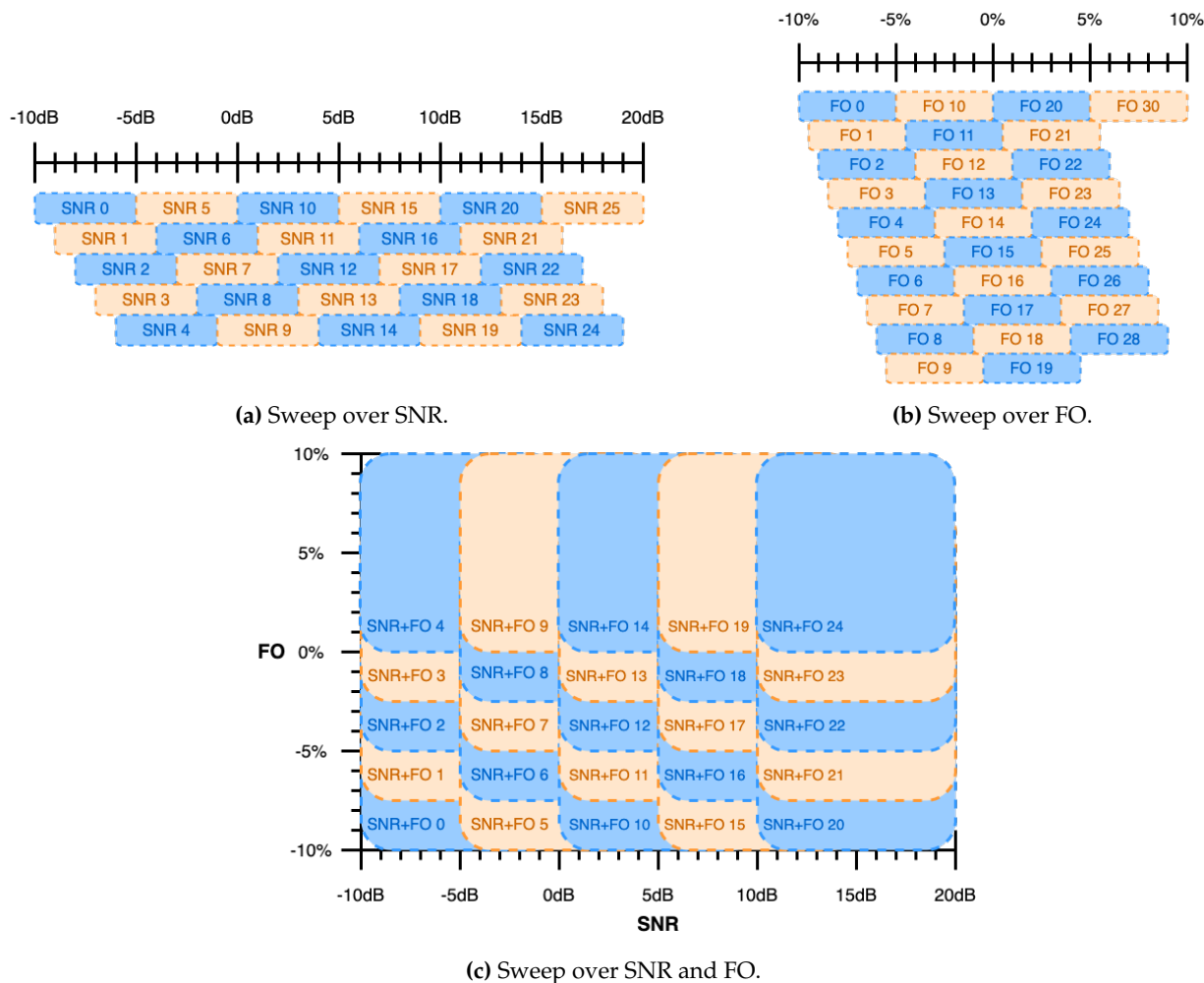


**Figure 5.** The parameter-of-interest range for each domain adaptation data subset.

bandwidths, or other baseband processing. We do inherently assume all signals are sampled at a sufficiently high rate to meet Nyquist’s sampling theorem. That is, the AWGN captures have a Nyquist rate of 1, and all other captures have a Nyquist rate of either 0.5 or 0.33 (twice or three times the Nyquist bandwidth). However, the AMC and TL approaches used herein do not rely on this critical sampling assumption, as there is no attempt to reconstruct the original signal.

### 3.1.2. The Master Dataset

The systematic evaluation of TL performance as a function of SNR, FO, and modulation type conducted in this work is possible through the construction of data-subsets with carefully selected metadata parameters from the larger master dataset. The constructed master dataset contains 600000 examples of each the signal types given in Table 1, for a total of 13.8 million examples. For each example, the SNR is selected uniformly at random between  $[-10\text{dB}, 20\text{dB}]$ , the FO is selected uniformly at random between  $[-10\%, 10\%]$  of the sample rate, and all further signal generation parameters relevant for the signal type, including symbol order, carrier spacing, modulation index, and filtering parameters (excess bandwidth, symbol overlap/filter delay, and/or beta), are selected uniformly at random from the ranges specified in Table 1. Each example and the associated metadata is saved in SigMF format [30].

### 3.1.3. The Sweep over SNR

To analyze the impact of SNR alone on TL performance, 26 source data-subsets were constructed from the larger master dataset using configuration files, as shown in Fig. 5a. Each data-subset contains examples with SNRs selected uniformly at random from a 5dB range sweeping from -10dB to 20dB in 1dB steps (i.e. [-10dB, -5dB], [-9dB, -4dB], ..., [15dB, 20dB]), and for each data-subset in this SNR sweep, FO was selected uniformly at random between [-5%, 5%] of sample rate. This SNR sweep yielded 26 pre-trained source models, each of which was transferred to the remaining 25 target data-subsets (as shown in Fig. 4b), yielding 650 models transferred using head re-training and 650 models transferred using fine-tuning. Additionally, 26 baseline models were trained, as described further in Section 3.2.

### 3.1.4. The Sweep over FO

To analyze the impact of FO alone on TL performance, 31 source data-subsets were constructed from the larger master dataset (as shown in Fig. 5b) containing examples with FOs selected uniformly at random from a 5% range sweeping from -10% of sample rate to 10% of sample rate in 0.5% steps (i.e. [-10%, -5%], [-9.5%, -4.5%], ..., [5%, 10%]). For each data-subset in this FO sweep, SNR was selected uniformly at random between [0dB, 20dB]. This FO sweep yielded 31 pre-trained source models, each of which was transferred to the remaining 30 target data-subsets (as shown in Fig. 4b) yielding 930 models transferred using head re-training, and 930 models transferred using fine-tuning. Additionally, 31 baseline models were trained, as described further in Section 3.2.

### 3.1.5. The Sweep over both SNR & FO

To analyze the impact of both SNR and FO on TL performance, 25 source data-subsets were constructed from the larger master dataset (as shown in Fig. 5c) containing examples with SNRs selected uniformly at random from a 10dB range sweeping from -10dB to 20dB in 5dB steps (i.e. [-10dB, 0dB], [-5dB, 5dB], ..., [10dB, 20dB]) and with FOs selected uniformly at random from a 10% range sweeping from -10% of sample rate to 10% of sample rate in 2.5% steps (i.e. [-10%, 0%], [-7.5%, 2.5%], ..., [0%, 10%]). This SNR and FO sweep yielded 25 pre-trained source models, each of which was transferred to the remaining 24 target data-subsets (as shown in Fig. 4b) yielding 600 models transferred using head re-training, and 600 models transferred using fine-tuning. Additionally, 25 baseline models were trained, as described further in Section 3.2.

### 3.1.6. Modulation Scheme Experiments

To analyze the impact of modulation type on TL performance, two groups of data-subsets were constructed. The first set of data-subsets aims to investigate TL performance across broad categories of modulation types, namely linear, frequency-shifted, and analog modulation schemes, as well as datasets containing combinations of modulation types. More specifically, 5 source data-subsets were constructed from the larger master dataset containing the following modulation schemes:

- All modulations
- Small Subset – BPSK, QPSK, OQPSK, QAM16, QAM64, APSK16, FSK 5k, MSK, FM-NB, DSB, USB, AWGN
- Linear modulations – BPSK, QPSK, PSK8, PSK16, OQPSK, QAM16, QAM32, QAM64, APSK16, APSK32, AWGN
- Frequency-shifted modulations – FSK 5k, FSK 75k, GFSK 5k, GFSK 75k, MSK, GMSK, AWGN
- Analog modulations – FM-NB, FM-WB, DSB, DSBSC, LSB, USB, AWGN

For each data-subset in this modulation type experiment, called “Modulation Experiment 1”, SNR was selected uniformly at random between [0dB, 20dB] and FO was selected uniformly at random between [-5%, 5%] of sample rate. This experiment yielded 5 pre-trained source models, each of which was transferred to the remaining 4 target data-subsets, yielding 20 models transferred using head re-training and 20 models transferred using fine-tuning. Additionally, 5 baseline models were trained, as described further in Section 3.2.

The second set of data-subsets was constructed such that a single modulation type was added/removed from the small/all modulations datasets described above, mimicking a successive model refinement scenario. More specifically, the 12 source data-subsets were constructed from the larger master dataset containing:

- small – BPSK, QPSK, OQPSK, QAM16, 64qam, APSK16, FSK 5k, MSK, FM-NB, DSB, USB, AWGN
- subset1 – small + PSK8
- subset2 – subset1 + PSK16
- subset3 – subset2 + QAM32
- subset4 – subset3 + APSK32
- subset5 – subset4 + FSK 75k
- subset6 – subset5 + GFSK 5k
- subset7 – subset6 + GFSK 75k
- subset8 – subset7 + GMSK
- subset9 – subset8 + FM-WB
- subset10 - subset9 + DSBSC
- all – subset10 + LSB

Again, SNR was selected uniformly at random between [0dB, 20dB] and FO was selected uniformly at random between [-5%, 5%] of sample rate. This experiment is called “Modulation Experiment 2” herein. This experiment yielded 12 pre-trained source models, each of which was transferred to the remaining 11 target data-subsets, yielding 132 models transferred using head re-training and 132 models transferred using fine-tuning. Additionally, 12 baseline models were trained, as described further in Section 3.2.

### 3.2. Model Architecture and Training

In this work, we utilize a single architecture trained across pairwise combinations of source/target datasets with varying (1) SNRs, (2) FOs, (3) SNRs and FO, or (4) modulation types in order to identify the impact of these parameters-of-interest on TL performance. Given the large number of models trained for this work, training time was a primary concern when selecting the model architecture. Therefore, this work uses a simple CNN architecture, shown in Table 2, that is based off of the architectures used in [23] and [31], with a reduction in the input size. Although many works including [23] and [31] have found success using larger input sequences, works such as [32] and [11] have found 128 input samples to be sufficient. Recognizing that longer input sequences results in increased computation and training time, in this work, 128 raw IQ samples are used as input corresponding to approximately 16-32 symbols depending on the symbol rate of the example. These samples are fed to the network in a (1, 2, 128) tensor, such that 1 refers to the number of channels, 2 refers to the IQ components, and 128 refers to the number of samples. The network contains two 2D convolutional layers, the first uses 1500 kernels of size (1,7) and the second uses 260 kernels of size (2,7). The second convolutional layer is followed by a flattening layer, a dropout layer using a rate of 0.5, and two linear fully-connected layers containing 65 and  $n$  nodes where  $n$  is the number of

**Table 2.** Model architecture with  $n$  being the number of output classes (modulation types) trained.

Layer Type	Num Kernels/Nodes	Kernel Size
Input	size = (2, 128)	
Conv2d	1500	(1, 7)
ReLU		
Conv2d	260	(2, 7)
ReLU		
Dropout	rate = 0.5	
Flatten		
Linear	65	
ReLU		
Linear	$n$	
Softmax		
Trainable Parameters: $7432725 + (66 \cdot n)$		

output classes (i.e. modulation schemes) being trained. Both convolutional layers and the first linear layer use a ReLU activation function, and the final linear layer uses a Softmax activation function.

The model pre-training and TL process is shown in Fig. 4b, and represents a standard training pipeline. For pre-training, the training dataset contained 5000 examples per class, and the validation dataset contained 500 examples per class. These dataset sizes are consistent with [23] and adequate to achieve consistent convergence. Each model was trained using the Adam optimizer [33] and Cross Entropy Loss [34], with the PyTorch default hyper-parameters [35] (a learning rate of 0.001, without weight decay), for a total of 100 epochs. A checkpoint was saved after the epoch with the lowest validation loss, and was reloaded at the conclusion of the 100 epochs.

This work examines both head re-training and model fine-tuning methods. For head re-training and model fine-tuning, the training dataset contained 500 examples per class, and the validation dataset contained 50 examples per class, representing a smaller sample of available target data. The head re-training and fine-tuning processes both used the Adam optimizer and Cross Entropy Loss as well, with checkpoints saved at the lowest validation loss. During head re-training, only the final layer of the model was trained, again using the PyTorch default hyper-parameters, while the rest of the model’s parameters were frozen. During fine-tuning, the entire model was trained with a learning rate of 0.0001, an order of magnitude smaller than the PyTorch default of 0.001. Finally, all baseline models were trained using the same training process as the pre-trained models, but with 500 training examples per class and 50 validation examples per class, as was used in the TL setting.

#### 4. Experimental Results & Analysis

The product of the experiments performed herein is 98 data subsets, each with distinct RF domains and tasks, corresponding baseline and source models trained from random initialization, and 4664 transfer learned models, half transferred using head re-training and the remaining half transferred using fine-tuning. Given the careful curation of the signal parameters contained within each data subset, as well as the breadth of signal types and parameters observed, generalized conclusions can be drawn regarding TL performance as a function of changes in the propagation environment (SNR), transmitter/receiver hardware (FO), and AMC task. However, it should be noted that further experiments using captured data are required in order to draw more concrete guidelines for using RF TL in the field [3], and is left for future

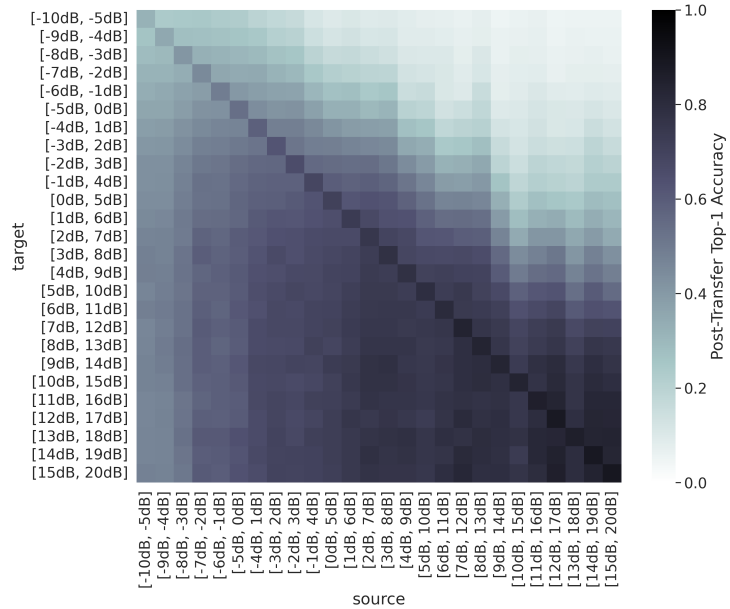


**Figure 6.** The post-transfer top-1 accuracy for each source/target dataset pair constructed for the sweep over SNR using head re-training to perform domain adaptation, shown on a scale of [0.0, 1.0]. When fine-tuning is used to perform domain adaptation, the same trends are apparent.

work. The following subsections present the results obtained from the experiments performed, and discuss insights and practical takeaways that can be gleaned from the results given.

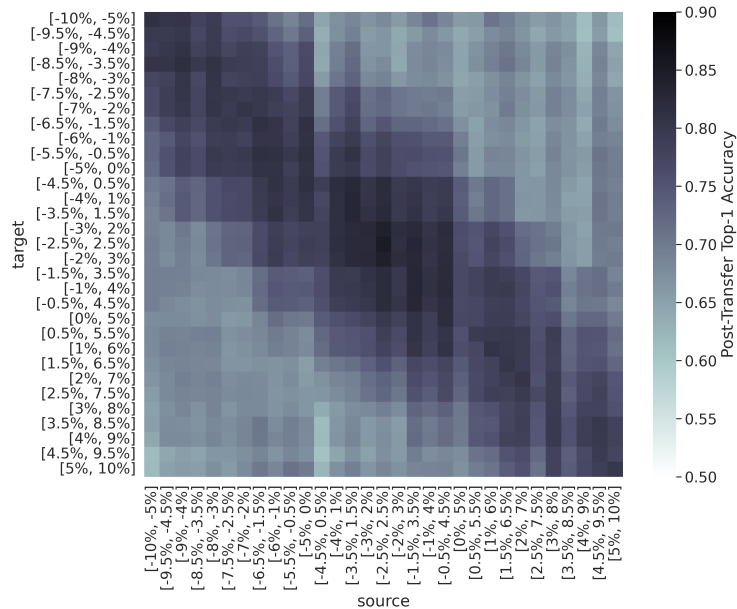


**Figure 7.** The post-transfer top-1 accuracy for each source/target dataset pair constructed for the sweep over FO using head re-training to perform domain adaptation, shown on a scale of [0.5, 0.9]. When fine-tuning is used to perform domain adaptation, the same trends are apparent.

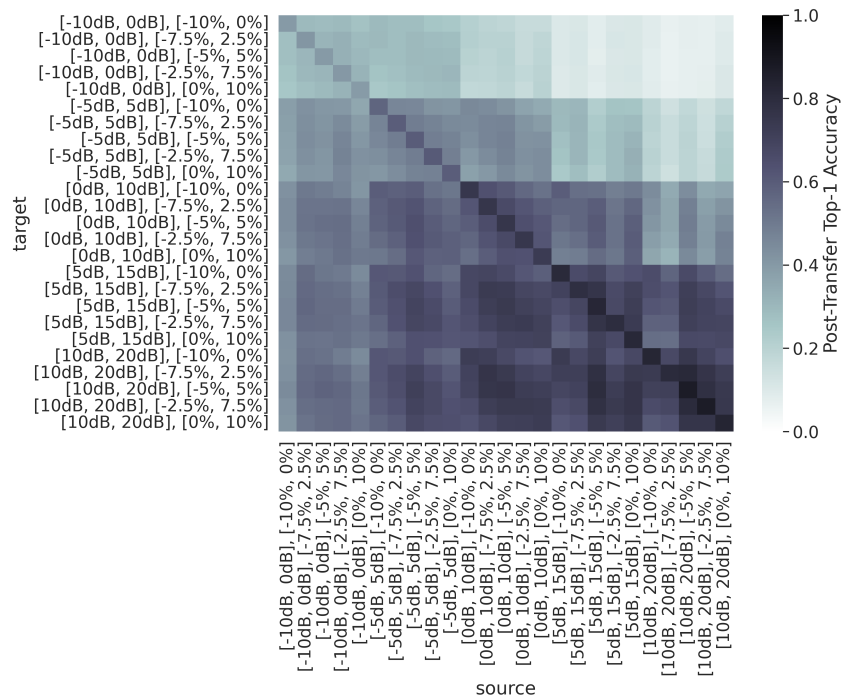


**Figure 8.** The post-transfer top-1 accuracy for each source/target dataset pair constructed for the sweep over both SNR and FO using head re-training to perform domain adaptation, shown on a scale of [0.0, 1.0]. When fine-tuning is used to perform domain adaptation, the same trends are apparent.

#### 4.1. When and How is RF Domain Adaptation most successful?

##### 4.1.1. Impact of Source/Target Domain Similarity and “Difficulty” on Transfer Performance

The heatmaps in Figs. 6–8 show the post-transfer top-1 accuracy achieved with each of the source/target pairs. Note that the post-transfer top-1 accuracy results shown in Figs. 6–8 are from the models that used head re-training to transfer from the source to target domains/datasets. However, the accuracy results from the models that used fine-tuning for transfer show the same trends.

Figs. 6–8 show that highest post-transfer performance is achieved along the diagonal of the heatmap, where the source and target domains are most similar. It should be noted that while the notion of domain similarity is ill-defined in general, for the purposes of this work, we are able to say that domains are more similar when the difference between the source and target SNR and/or FO ranges is smaller, as all other data generation parameters are held constant. These trends are expected, as models trained on similar domains likely learn similar features, and is consistent with the general theory of TL [12], as well as existing works in modalities outside of RF [36].

Figs. 6–8 also show that transfer across changes in FO is approximately symmetric, while transfer across changes in SNR are not. This behavior is also expected, and can be attributed to changes in the relative “difficulty” between the source and target domains. More specifically, changing the source/target SNR inherently changes the difficulty of the problem, as performing AMC in lower SNR channel environments is more challenging than performing AMC in high SNR channel environments. Therefore, the source models trained on the lower SNR ranges will transfer to the higher SNR ranges, though may not perform optimally, while the source models trained on the higher SNR ranges will fail to transfer to the lower SNR ranges, as shown in Figs. 6 and 8. In contrast, changing the source/target FO does not make performing AMC any more

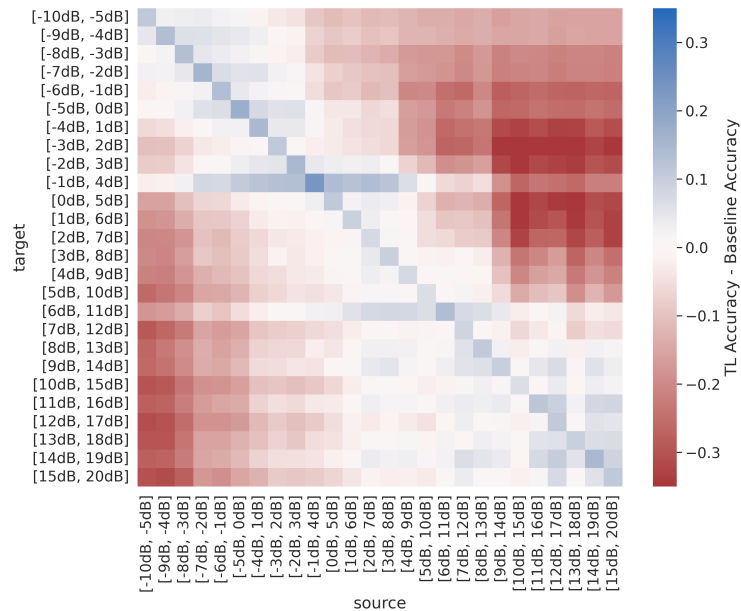


**Figure 9.** The difference between post-transfer top-1 accuracy and target baseline accuracy for the sweep over SNR using head re-training, shown on a scale of  $[-0.35, 0.35]$ . When fine-tuning is used to perform domain adaptation, the same trends are apparent. Note that the increase in performance when the source and target are the same (i.e. along the diagonal) is due to the 10x increase in training data between the baseline and pre-trained models.

or less difficult, but may require modifications to the learned features to accommodate which can be likened to performing FO calibration, as is standard practice in RF receiver operations. Consequently, small changes in FO,  $\omega_{\Delta}[t]$ , in either the positive and negative direction, are expected to perform similarly. Figure 7 indeed shows that TL performance is approximately symmetric, with best performance closest to the diagonal where the source and target FO ranges are most closely aligned.

Practically, these trends indicate that the effectiveness of RF domain adaptation increases as the source and target domains become more and more similar, and, when applicable, RF domain adaptation is more often successful when transferring from harder to easier domains when compared to transferring from easier to harder domains. For example, transferring from  $[-5\text{dB}, 0\text{dB}]$  to  $[0\text{dB}, 5\text{dB}]$  SNR is likely more effective than transferring from  $[5\text{dB}, 10\text{dB}]$  to  $[0\text{dB}, 5\text{dB}]$  SNR because although the similarity of between datasets in these two transfer scenarios is the same,  $[-5\text{dB}, 0\text{dB}]$  is a more challenging domain than  $[0\text{dB}, 5\text{dB}]$  whereas  $[5\text{dB}, 10\text{dB}]$  is an easier domain than  $[0\text{dB}, 5\text{dB}]$ . However, transferring from a FO range of  $[-9\%, -4\%]$  of sample rate to  $[-8\%, -3\%]$  of sample rate is likely more effective than transferring from a FO range of  $[-10\%, -5\%]$  of sample rate to  $[-8\%, -3\%]$  of sample rate because  $[-9\%, -4\%]$  of sample rate and  $[-8\%, -3\%]$  of sample rate are more similar than  $[-10\%, -5\%]$  of sample rate and  $[-8\%, -3\%]$  of sample rate.

#### 4.1.2. Environment Adaptation vs. Platform Adaptation

Recalling that the sweep over SNR can be regarded as an environment adaptation experiment and the sweep over FO can be regarded as a platform adaptation experiment, more general conclusions can be drawn regarding the challenges that environment and platform adaptation present. From the discussion in the previous subsection regarding the impact that SNR and FO have on the relative difficulty of the AMC task, it follows that changes in

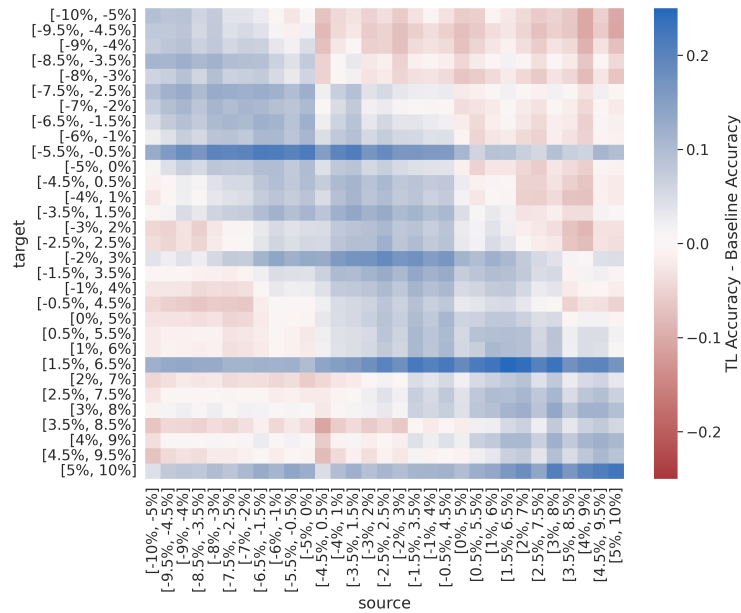


**Figure 10.** The difference between post-transfer top-1 accuracy and target baseline accuracy for the sweep over FO using head re-training, shown on a scale on  $[-0.25, 0.25]$ . When fine-tuning is used to perform domain adaptation, the same trends are apparent. Note that the increase in performance when the source and target are the same (i.e. along the diagonal) is due to the 10x increase in training data between the baseline and pre-trained models.

SNR are likely more challenging to overcome than changes in FO. That is, changes in channel environment are more challenging to overcome using TL techniques than changes in transmitter/receiver hardware, such that environment adaptation is more difficult to achieve than platform adaptation. While this trend is indirectly shown through the range of accuracies achieved in Figs. 6-8, which is smaller for the FO sweep than the SNR sweep and SNR + FO sweep, and is more directly shown in Figs. 9 and 10.

Figs. 9 and 10 present the difference between post-transfer top-1 accuracy and target baseline accuracy for the SNR and FO sweeps, such that when the difference value is positive the TL model outperforms the baseline model and vice versa. These results show that for the sweep over SNR, the TL model only outperforms the baseline near the diagonal where the source and target are very similar. However, for the sweep over FO, the TL model outperforms the baseline for a greater number of source/target pairs.

From these results, we can conclude that in practice TL is more useful for overcoming platform discrepancies than channel discrepancies, unless the channel discrepancy is small. If the channel discrepancy between source and target is large, one might consider simply training for random initialization on the target data to achieve top performance. Furthermore, if choosing a source dataset/model for a given target domain/task, one should consider the similarity of the source/target channel environment before the similarity of the source/target platform, as changes in transmitter/receiver pair are more easily overcome during TL.

#### 4.1.3. Head Re-Training vs. Fine-Tuning

Figs. 11 - 13 plot the difference between post-transfer top-1 accuracies achieved using head re-training versus fine-tuning such that positive values correspond to better fine-tuning performance and negative values correspond to better head re-training performance. These figures indicate that head re-training is as effective, if not more effective, than fine-tuning

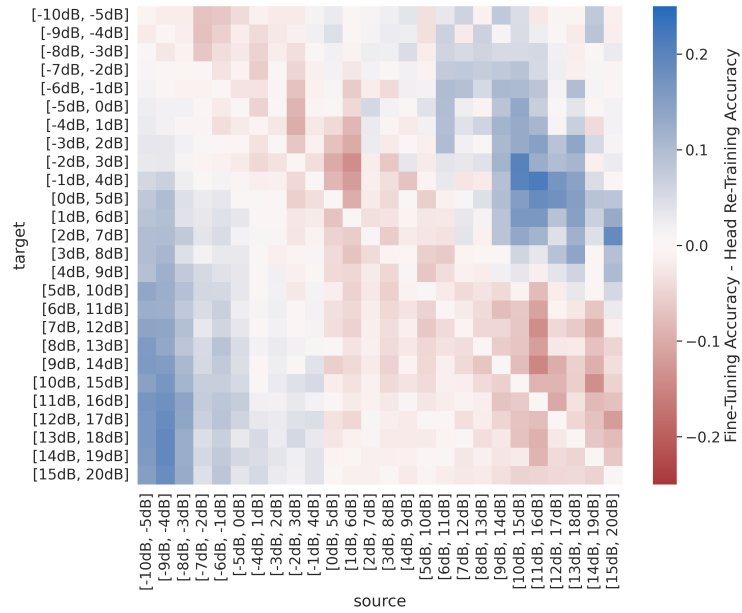


**Figure 11.** The difference between post-transfer top-1 accuracies achieved using head re-training versus fine-tuning for the sweep over SNR, shown on a scale of [-0.25, 0.25]. When the value is positive, fine-tuning outperforms head re-training. When the value is negative, head re-training outperforms fine-tuning.

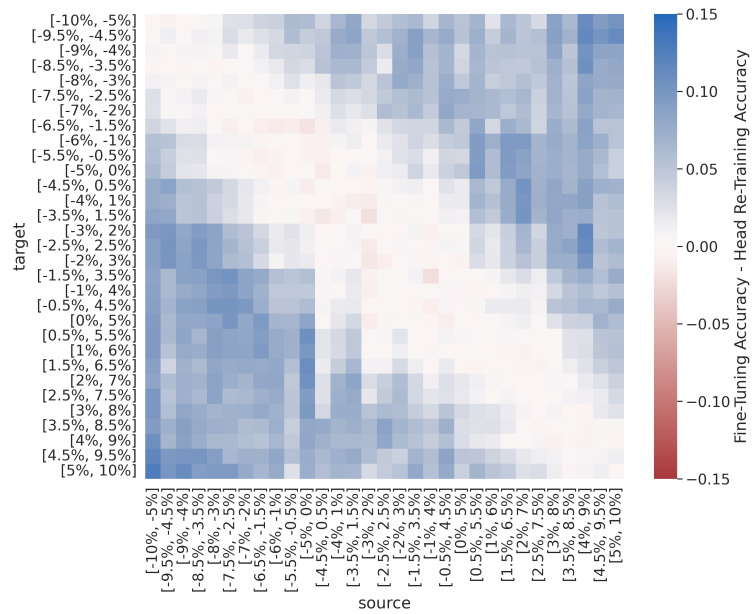


**Figure 12.** The difference between post-transfer top-1 accuracies achieved using head re-training versus fine-tuning for the sweep over FO, shown on a scale of [-0.15, 0.15]. When the value is positive, fine-tuning outperforms head re-training. When the value is negative, head re-training outperforms fine-tuning.

when the source and target domains are similar. Meanwhile, fine-tuning is more effective when the source and target domains are more dissimilar. Intuitively, this means that when the source/target domains are dissimilar, the features found in the early layers of the source model

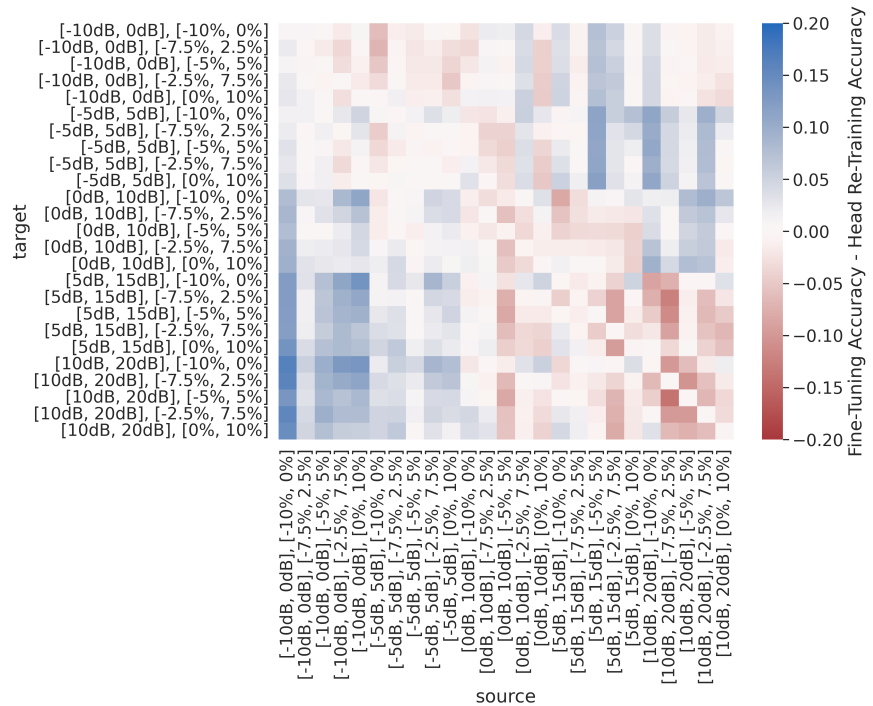


**Figure 13.** The difference between post-transfer top-1 accuracies achieved using head re-training versus fine-tuning for the sweep over SNR and FO, shown on a scale of  $[-0.2, 0.2]$ . When the value is positive, fine-tuning outperforms head re-training. When the value is negative, head re-training outperforms fine-tuning.

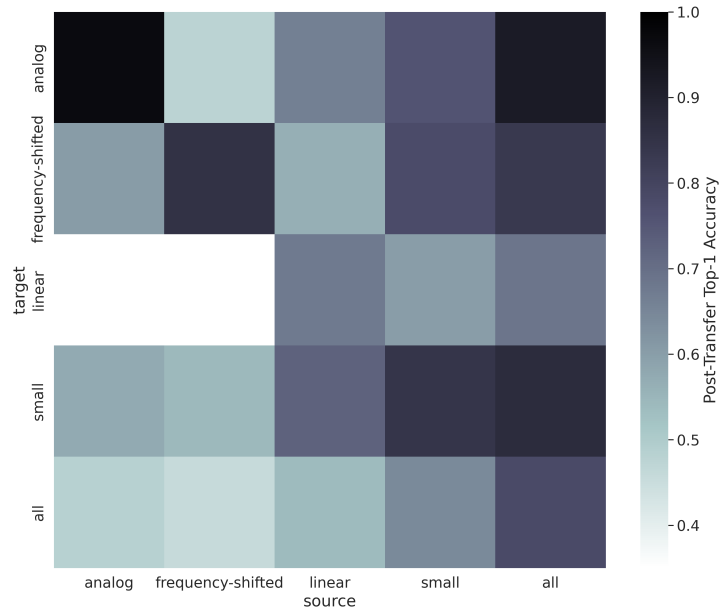
needed modification to discern between modulation types in the target domain. However, recalling that Figs. 9 and 10 showed TL only provides benefit when the source and target are somewhat similar, we can conclude that head re-training is as effective, if not more effective, than fine-tuning in the settings where TL increases performance over the baseline. Given that head re-training is more time efficient and less computationally expensive than fine-tuning, there is a strong case for using head re-training over fine-tuning when performing RF domain adaptation.

#### 4.2. When and How is RF Sequential Learning Most Successful?

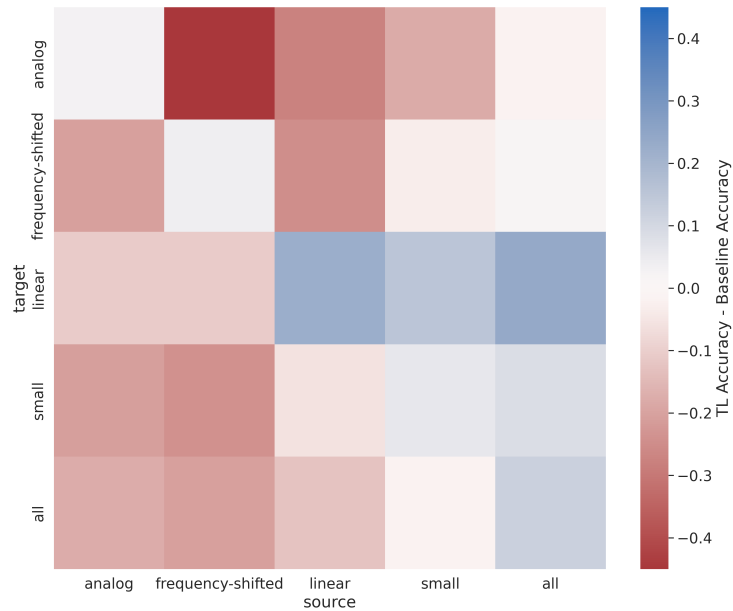
##### 4.2.1. Sequential Learning Across Signal Types: Modulation Experiment 1

Fig. 14 shows the post-transfer top-1 accuracy for each source/target dataset in Modulation Experiment 1. As in the domain adaptation experiments discussed previously, the best transfer generally occurs along the diagonal of the heatmap, where the source/target similarity is highest. Additionally, the subsets containing only a single type of modulation scheme (i.e. the analog, frequency-shifted, linear subsets) don't transfer well between one another, and also don't transfer well to the subsets which contain multiple types of modulation schemes (i.e. the small and all subsets). Meanwhile, the small and all subsets transfer fairly well to the analog, frequency-shifted, and linear subsets. These results are verified by the results shown in Fig. 15 which presents the difference between post-transfer top-1 accuracy and the baseline target models, and shows that TL only increases performance over the baseline models when there is significant overlap between the modulation schemes in each subset.

These results are expected when we consider the general setting in which TL is beneficial: when the source and target are "similar". When no similar signal types between source/target



**Figure 14.** The post-transfer top-1 accuracy for each source/target dataset pair constructed for Modulation Experiment 1 using head re-training, shown on a scale of [0.35, 1.0]. When fine-tuning is used, the same trends are apparent.



**Figure 15.** The difference between post-transfer top-1 accuracy and target baseline accuracy for Modulation Experiment 1 using head re-training, shown on a scale of [-0.45, 0.45]. When fine-tuning is used, the same trends are apparent. Note that the increase in performance when the source and target are the same (i.e. along the diagonal) is due to the 10x increase in training data between the baseline and pre-trained models.

there is little-to-no benefit to using TL, such as when attempting transfer between the analog, frequency-shifted, and linear subsets. However, because the small and all subsets contain at

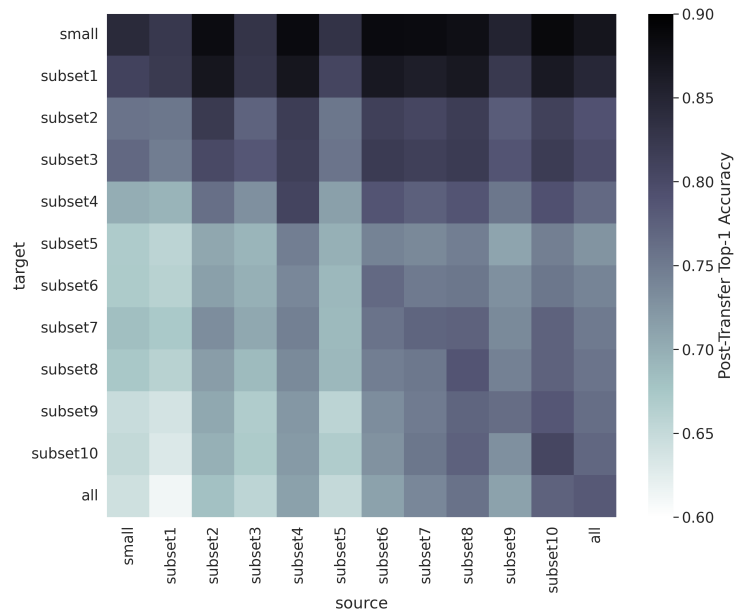


**Figure 16.** The post-transfer top-1 accuracy for each source/target dataset pair constructed for Modulation Experiment 2 using head re-training, shown on a scale of [0.6, 0.9]. When fine-tuning is used, the same trends are apparent.

least one modulation scheme from each of the analog, frequency-shifted, and linear subsets, the pre-trained source model has some prior knowledge of each category of modulation schemes from which to build. Practically, these results indicate that TL is only beneficial when similar signal types in the source and target datasets.

#### 4.2.2. Sequential Learning For Successive Model Refinement: Modulation Experiment 2

Figs. 16 and 17 present the post-transfer top-1 accuracy and the difference between the post-transfer top-1 accuracy for Modulation Experiment 2 and target baseline accuracy for Modulation Experiment 2 respectively. These results indicate that it is easier to remove output classes during the TL phase than it is to add output classes, as evidenced by higher performance in the upper triangle of the heatmap in Fig. 16, as well as the significant performance benefits over the target baseline models shown in Fig. 17. This behavior is expected, as, intuitively, it is easier to forget or disregard prior knowledge than to acquire new knowledge during transfer. More specifically, by pre-training on a larger subset of signal types (i.e. outputs), the source model has already learned features to identify all of the modulation classes in the target task. In fact, the source model has likely learned more features than necessary to perform the target task, and could undergo feature pruning in order to reduce computational complexity. It should also be noted that the task gets easier as output classes are removed, further contributing to the trend. Practically, these results dictate that one should utilize a source task that encompasses the target task, when possible.

#### 4.2.3. Head Re-training vs. Fine Tuning

Finally, Figs. 18 and 19 present the difference between post-transfer top-1 accuracies achieved using head re-training versus fine-tuning for Modulation Experiments 1 and 2 respectively. These results show that fine-tuning outperforms head re-training in all cases where the source/target tasks are 'less similar.' Meanwhile, when the source/target subsets have some modulation schemes in common, head re-training outperforms fine-tuning. However, as was

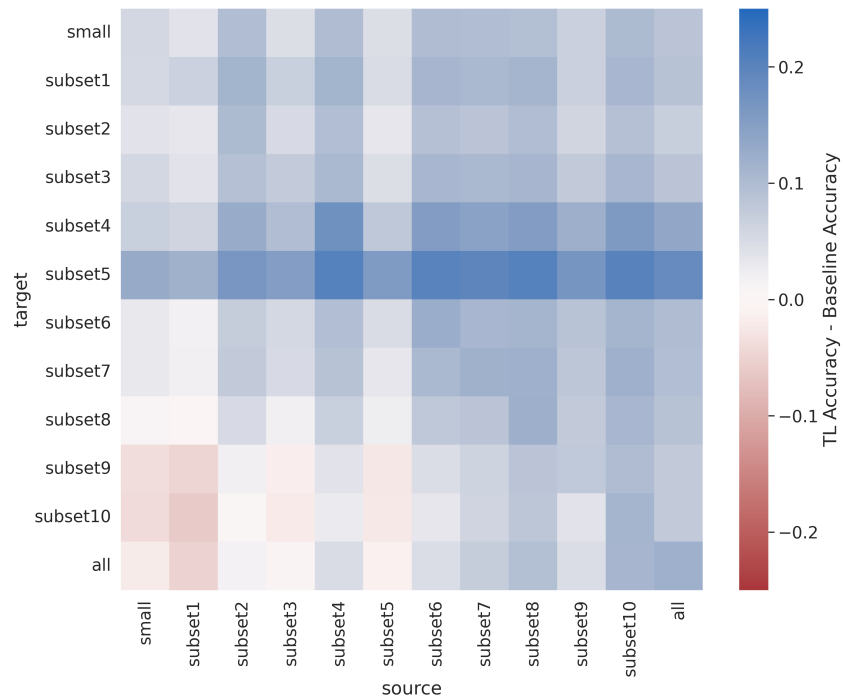


**Figure 17.** The difference between post-transfer top-1 accuracy and target baseline accuracy for Modulation Experiment 2 using head re-training, shown on a scale of  $[-0.25, 0.25]$ . When fine-tuning is used, the same trends are apparent. Note that the increase in performance when the source and target are the same (i.e. along the diagonal) is due to the 10x increase in training data between the baseline and pre-trained models.

the case in the domain adaptation experiments discussed in Section 4.1.3, head re-training is as effective, if not more effective, than fine-tuning in the settings where TL increases performance over the baseline. Therefore, head re-training is the preferred method of performing RF sequential learning as well, as head re-training is generally more time efficient and less computationally expensive than fine-tuning.

## 5. Conclusion

TL has yielded tremendous performance benefits in CV and NLP, and as a result, TL is all but commonplace in these fields. However, the benefits of TL have yet to be fully demonstrated and integrated in RFML. To begin to address this deficit, this work systematically evaluated RF TL performance as a function of SNR, FO, and modulation type for an AMC use-case. Through this exhaustive study, a number of guidelines have been identified for when and how to use RF TL successfully. More specifically, results indicate:

- Using source models trained on the most similar domain/task to the target yields highest performance
- Transferring from a more challenging domain/task than the target, is preferred to transferring from an easier domain/task
- Selecting source models based on the similarity of the source/target channel environment is more important than the similarity of the source/target platform(s)

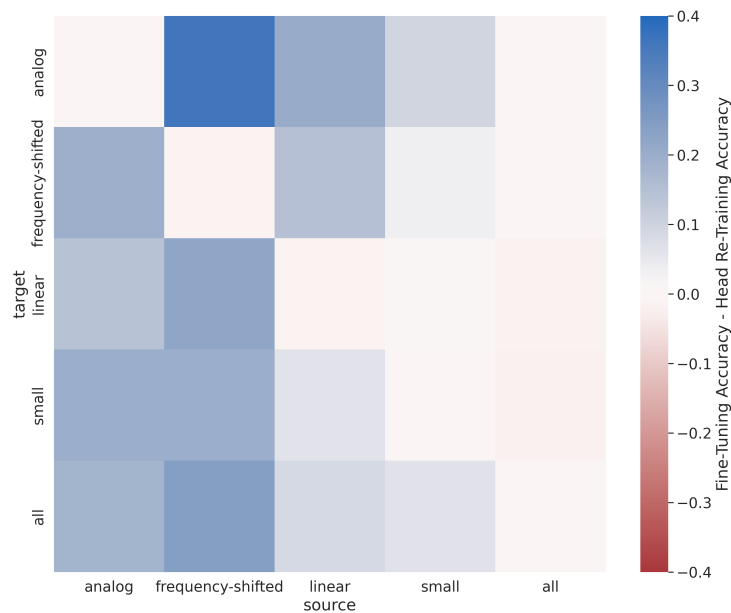


**Figure 18.** The difference between post-transfer top-1 accuracies achieved using head re-training versus fine-tuning for Modulation Experiment 1, shown on a scale of  $[-0.4, 0.4]$ . When the value is positive, fine-tuning outperforms head re-training. When the value is negative, head re-training outperforms fine-tuning.

- Head re-training generally provides the highest performance in any RF TL case where TL provides a performance benefit over training from random initialization, as measured by post-transfer top-1 accuracy, time efficiency, and computational complexity.

As previously mentioned these initial guidelines are subject to further experimentation using additional signal types, channel models, use-cases, model architectures, and augmented or captured datasets. Continuing and extending the analysis conducted herein will provide a more thorough understanding of RF TL behavior and performance across a wider range of use-cases and deployment settings. Further experimentation should include:

- An analysis of multi-task learning behavior using synthetic and/or captured data
- Analyses of RF TL performance across other metadata parameters-of-interest such as fading/multi-path channel environments, sample rate, IQ imbalance, etc.
- Analyses of TL performance for other RFML use-cases such as SEI, signal detection, etc.
- An analysis of RF TL techniques for transferring between use-cases. For example, can sequential learning techniques be used to transfer between AMC and SEI use-cases? Is multi-task learning better suited to performing this type of transfer?
- Analyses of RF TL performance across varying domains/tasks using captured data
- An analysis of RF TL performance across synthetic, augmented, and captured datasets

Provided future verification and refinement of these results and guidelines, these guidelines can be used in future RFML systems to construct the highest performing models for a given target domain when data is limited. More specifically, these guidelines begin a discussion regarding how best to continually update RFML models once deployed, in an online or incremental fashion, to overcome the highly fluid nature of modern communication systems [2].

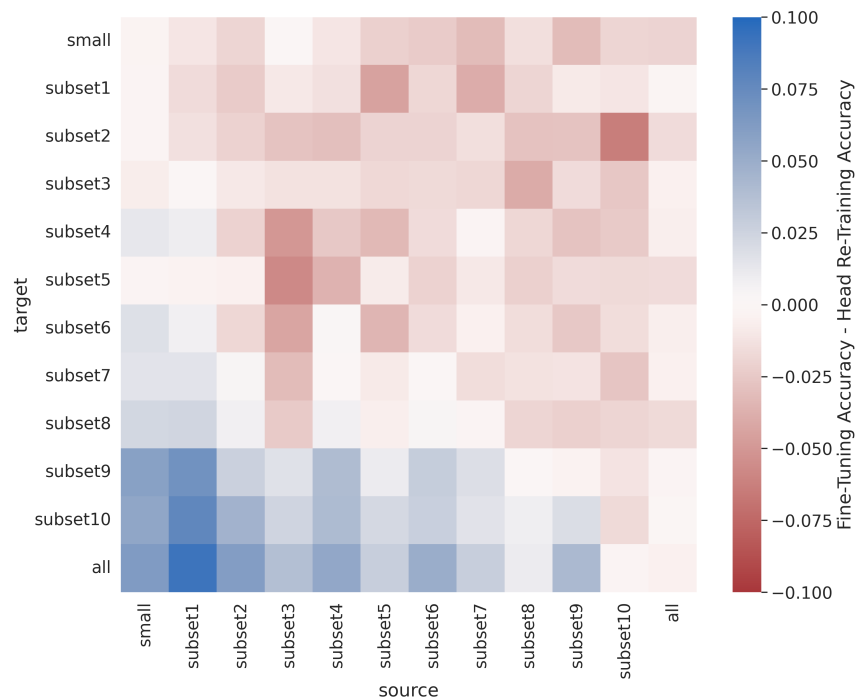


**Figure 19.** The difference between post-transfer top-1 accuracies achieved using head re-training versus fine-tuning for Modulation Experiment 2, shown on a scale of  $[-0.1, 0.1]$ . When the value is positive, fine-tuning outperforms head re-training. When the value is negative, head re-training outperforms fine-tuning.

**Author Contributions:** Conceptualization, Lauren J. Wong; methodology, Lauren J. Wong, Sean McPherson, and Alan J. Michaels; software, Lauren J. Wong; validation, Lauren J. Wong, Sean McPherson, and Alan J. Michaels; formal analysis, Lauren J. Wong; investigation, Lauren J. Wong; resources, Sean McPherson; data curation, Lauren J. Wong; writing—original draft preparation, Lauren J. Wong; writing—review and editing, Sean McPherson and Alan J. Michaels; visualization, Lauren J. Wong; supervision, Sean McPherson and Alan J. Michaels; project administration, Sean McPherson and Alan J. Michaels; funding acquisition, Not Applicable. All authors have read and agreed to the published version of the manuscript.

**Funding:** This research received no external funding.

**Institutional Review Board Statement:** Not applicable.

**Informed Consent Statement:** Not applicable.

**Data Availability Statement:** The dataset used in this work is publicly available on IEEE DataPort at <https://iee-dataport.org/open-access/transfer-learning-rf-domain-adaptation-%E2%80%93-synthetic-dataset>.

**Conflicts of Interest:** The authors declare no conflict of interest.

### Abbreviations

The following abbreviations are used in this manuscript:

AM-DSB      amplitude modulation, double-sideband

AM-DSBSC    amplitude modulation, double-sideband suppressed-carrier

AM-LSB      amplitude modulation, lower-sideband

---

AM-USB	amplitude modulation, upper-sideband
AMC	automatic modulation classification
APSK16	amplitude and phase-shift keying, order 16
APSK32	amplitude and phase-shift keying, order 32
AWGN	additive white Gaussian noise
BPSK	binary phase-shift keying
CLDNN	convolutional long-short term deep neural network
CNN	convolutional neural network
CV	computer vision
DARPA	Defense Advanced Research Projects Agency
DL	deep learning
DNN	deep neural network
FM-NB	narrow band frequency modulation
FM-WB	wide band frequency modulation
FO	frequency offset
FSK5k	frequency-shift keying, 5kHz carrier spacing
FSK75k	frequency-shift keying, 75kHz carrier spacing
GFSK5k	Gaussian frequency-shift keying, 5kHz carrier spacing
GFSK75k	Gaussian frequency-shift keying, 75kHz carrier spacing
GMSK	Gaussian minimum-shift keying
IQ	in-phase/quadrature
LEEP	Log Expected Empirical Prediction
LogME	Logarithm of Maximum Evidence
LSTM	Long Short-Term Memory
ML	machine learning
MLP	multi-layer perceptrons
MSK	minimum-shift keying
NLP	natural language processing
NN	neural network
OQPSK	offset quadrature phase-shift keying
PSK16	phase-shift keying, order 16
PSK8	phase-shift keying, order 8
QAM16	quadrature amplitude modulation, order 16

QAM32	quadrature amplitude modulation, order 32
QAM64	quadrature amplitude modulation, order 64
QPSK	quadrature phase-shift keying
RF	radio frequency
RFML	radio frequency machine learning
RNN	Recurrent Neural Network
RRC	root-raised cosine
SEI	specific emitter identification
SNR	signal-to-noise ratio
TL	transfer learning

## References

- Morocho-Cayamcela, M.E.; Lee, H.; Lim, W. Machine Learning for 5G/B5G Mobile and Wireless Communications: Potential, Limitations, and Future Directions. *IEEE Access* **2019**, *7*, 137184–137206. <https://doi.org/10.1109/ACCESS.2019.2942390>.
- Wong, L.J.; Clark, W.H.; Flowers, B.; Buehrer, R.M.; Headley, W.C.; Michaels, A.J. An RFML Ecosystem: Considerations for the Application of Deep Learning to Spectrum Situational Awareness. *IEEE Open Journal of the Communications Society* **2021**, *2*, 2243–2264. <https://doi.org/10.1109/OJCOMS.2021.3112939>.
- Clark IV, W.H.; Hauser, S.; Headley, W.C.; Michaels, A.J. Training data augmentation for deep learning radio frequency systems. *The Journal of Defense Modeling and Simulation* **2021**, *18*, 217–237.
- Hauser, S.C. Real-World Considerations for Deep Learning in Spectrum Sensing. Master's thesis, Virginia Tech, 2018.
- Sankhe, K.; Belgiovine, M.; Zhou, F.; Riyaz, S.; Ioannidis, S.; Chowdhury, K. ORACLE: Optimized Radio Classification through Convolutional Neural Networks. In Proceedings of the IEEE INFOCOM 2019-IEEE Conference on Computer Communications. IEEE, 2019, pp. 370–378.
- Ruder, S. Neural transfer learning for natural language processing. PhD thesis, NUI Galway, 2019.
- Olivas, E.S.; Guerrero, J.D.M.; Martinez-Sober, M.; Magdalena-Benedito, J.R.; Serrano, L.; et al. *Handbook of research on machine learning applications and trends: Algorithms, methods, and techniques*; IGI Global, 2009.
- Wong, L.J.; Michaels, A.J. Transfer Learning for Radio Frequency Machine Learning: A Taxonomy and Survey. *Sensors* **2022**, *22*. <https://doi.org/10.3390/s22041416>.
- Rondeau, T. Radio Frequency Machine Learning Systems (RFMLS).
- Dobre, O.A.; Abdi, A.; Bar-Ness, Y.; Su, W. Survey of automatic modulation classification techniques: classical approaches and new trends. *IET Communications* **2007**, *1*, 137–156.
- West, N.E.; O'Shea, T. Deep architectures for modulation recognition. In Proceedings of the 2017 IEEE Int. Symp. on Dynamic Spectrum Access Networks (DySPAN), 2017, pp. 1–6.
- Pan, S.J.; Yang, Q. A Survey on Transfer Learning. *IEEE Trans. on Knowledge and Data Eng.* **2010**, *22*, 1345–1359. <https://doi.org/10.1109/TKDE.2009.191>.
- Chen, S.; Zheng, S.; Yang, L.; Yang, X. Deep Learning for Large-Scale Real-World ACARS and ADS-B Radio Signal Classification. *IEEE Access* **2019**, *7*, 89256–89264. <https://doi.org/10.1109/ACCESS.2019.2925569>.
- Pati, B.M.; Kaneko, M.; Taparugssanagorn, A. A Deep Convolutional Neural Network Based Transfer Learning Method for Non-Cooperative Spectrum Sensing. *IEEE Access* **2020**, *8*, 164529–164545. <https://doi.org/10.1109/ACCESS.2020.3022513>.
- Kuzdeba, S.; Robinson, J.; Carmack, J. Transfer Learning with Radio Frequency Signals. In Proceedings of the 2021 IEEE 18th Annual Consumer Communications Networking Conference (CCNC), 2021, pp. 1–9. <https://doi.org/10.1109/CCNC49032.2021.9369550>.
- Robinson, J.; Kuzdeba, S. RiftNet: Radio Frequency Classification for Large Populations. In Proceedings of the 2021 IEEE 18th Annual Consumer Communications Networking Conference (CCNC), 2021, pp. 1–6. <https://doi.org/10.1109/CCNC49032.2021.9369455>.
- O'Shea, T.J.; Roy, T.; Clancy, T.C. Over-the-Air Deep Learning Based Radio Signal Classification. *IEEE Journal of Selected Topics in Signal Processing* **2018**, *12*, 168–179. <https://doi.org/10.1109/JSTSP.2018.2797022>.
- Dörner, S.; Cammerer, S.; Hoydis, J.; t. Brink, S. Deep Learning Based Communication Over the Air. *IEEE Journal of Selected Topics in Signal Processing* **2018**, *12*, 132–143. <https://doi.org/10.1109/JSTSP.2017.2784180>.
- Zheng, S.; Chen, S.; Qi, P.; Zhou, H.; Yang, X. Spectrum sensing based on deep learning classification for cognitive radios. *China Comm.* **2020**, *17*, 138–148. <https://doi.org/10.23919/JCC.2020.02.012>.

20. Clark, B.; Leffke, Z.; Headley, C.; Michaels, A. Cyborg Phase II Final Report. Technical report, Ted and Karyn Hume Center for National Security and Technology, 2019.
21. Peng, Q.; Gilman, A.; Vasconcelos, N.; Cosman, P.C.; Milstein, L.B. Robust Deep Sensing Through Transfer Learning in Cognitive Radio. *IEEE Wireless Comm. Letters* **2020**, *9*, 38–41. <https://doi.org/10.1109/LWC.2019.2940579>.
22. Ye, N.; Li, X.; Yu, H.; Zhao, L.; Liu, W.; Hou, X. DeepNOMA: A Unified Framework for NOMA Using Deep Multi-Task Learning. *IEEE Trans. on Wireless Comm.* **2020**, *19*, 2208–2225. <https://doi.org/10.1109/TWC.2019.2963185>.
23. Clark, W.H.; Arndorfer, V.; Tamir, B.; Kim, D.; Vives, C.; Morris, H.; Wong, L.; Headley, W.C. Developing RFML Intuition: An Automatic Modulation Classification Architecture Case Study. In Proceedings of the 2019 IEEE Military Comm. Conference (MILCOM), 2019, pp. 292–298. <https://doi.org/10.1109/MILCOM47813.2019.9020949>.
24. Wong, L.J.; McPherson, S. Explainable Neural Network-based Modulation Classification via Concept Bottleneck Models. In Proceedings of the 2021 IEEE Computing and Comm. Workshop and Conference (CCWC), 2021.
25. Clark IV, W.H.; Hauser, S.; Headley, W.C.; Michaels, A.J. Training Data Augmentation for Deep Learning Radio Frequency Systems. *JDMS Special Issue* **2021**.
26. Merchant, K. Deep Neural Networks for Radio Frequency Fingerprinting. PhD thesis, 2019.
27. Liu, Z.; Lian, T.; Farrell, J.; Wandell, B.A. Neural network generalization: The impact of camera parameters. *IEEE Access* **2020**, *8*, 10443–10454.
28. Gaeddert, J. liquid-dsp.
29. Wong, L.J.; McPherson, S.; Michaels, A.J. Transfer Learning for RF Domain Adaptation – Synthetic Dataset, 2022.
30. Hilburn, B.; West, N.; O’Shea, T.; Roy, T. SigMF: the signal metadata format. In Proceedings of the Proceedings of the GNU Radio Conference, 2018, Vol. 3.
31. Wong, L.J.; McPherson, S. Explainable Neural Network-based Modulation Classification via Concept Bottleneck Models. In Proceedings of the 2021 IEEE 11th Annual Computing and Communication Workshop and Conference (CCWC), 2021, pp. 0191–0196. <https://doi.org/10.1109/CCWC51732.2021.9376108>.
32. O’Shea, T.J.; Corgan, J.; Clancy, T.C. Convolutional radio modulation recognition networks. In Proceedings of the International conference on engineering applications of neural networks. Springer, 2016, pp. 213–226.
33. Kingma, D.P.; Ba, J. Adam: A method for stochastic optimization. *arXiv preprint arXiv:1412.6980* **2014**.
34. Cross Entropy Loss.
35. Paszke, A.; Gross, S.; Massa, F.; Lerer, A.; Bradbury, J.; Chanan, G.; Killeen, T.; Lin, Z.; Gimelshein, N.; Antiga, L.; et al. PyTorch: An imperative style, high-performance deep learning library. *Advances in neural information processing systems* **2019**, *32*, 8026–8037.
36. Rosenstein, M.T.; Marx, Z.; Kaelbling, L.P.; Dietterich, T.G. To transfer or not to transfer. In Proceedings of the NIPS 2005 workshop on transfer learning, 2005, Vol. 898, pp. 1–4.